

## THE EFFECT OF THE ELECTRIC FIELD ON THE NEMATIC LIQUID CRYSTAL MOLECULAR REDISTRIBUTION IN THE VICINITY OF AN IMMERSSED SPHEROCYLINDRICAL NANOPARTICLE

C. BERLIC, M. MOISESCU, V. BARNA\*

*University of Bucharest, Faculty of Physics, PO Box Mg-11, 077125, Bucharest, Romania*

We report a Monte Carlo simulation based on the Lebwohl-Lasher model for characterizing the molecular director configuration in a nematic liquid crystal having a spherocylindrical particle immersed inside. We describe the molecular orientation and spatial behavior of the order parameter and we retrieve the presence of a disclination line with the shape of the Saturn ring defect. By applying an electric field, the order inside the simulation cell is considerably changed and we find that the plane of the disclination line is moved perpendicular to the field direction. As the intensity of the field is increased the disclination line eventually disappears, the order inside the cell becoming uniaxial.

(Received July 10, 2012; Accepted September 14, 2012)

*Keywords:* Nematic liquid crystals, Monte Carlo simulation, Lebwohl-Lasher model, Order parameter, Biaxiality, Field order parameter

### 1. Introduction

Liquid crystalline materials (LCs) possess peculiar physical properties and have been proven as an excellent host system for testing many complex structures and even exotic phenomena. They own mechanical properties of a liquid, such as high fluidity (inability to support shear) while, simultaneously, exhibiting anisotropic behavior similar to a crystalline solid - in their optical, electrical, and magnetic properties [1,2]. Due to their unique mechanical and optical characteristics, liquid crystals are of considerable importance. Because of the large number of potential applications in the fields of science and technology, this class of materials have drawn the attention of scientists dealing with fundamental research topics, as well as applied physical, engineering and hi-tech issues [3-5].

The physical behavior of liquid crystals is highly influenced by the surface properties and, predominantly, the surface anchoring energies have a decisive role in establishing the local direction of the molecules [1,2]. These challenging phenomena make rather difficult a precise theoretical description of such systems and often is required the use of quite complex calculus, involving more sophisticated numerical methods, such as finite element method with an adaptive [6], or a moving mesh [7].

Another way of describing the orientational order and the properties of liquid crystals is by using computer simulations. Two major approaches exist for predicting the evolution of a system: the Monte Carlo (MC) method and Molecular Dynamics (MD) method [8-11]. MD simulations use a deterministic approach, based on a set of equations of motion, provided by the Hamiltonian of the system. MC method spawns new configurations in a random manner, but only accepts those which satisfy some definite criteria. A selection algorithm allows then for computing the thermodynamic averages.

Computer simulation is a well established method for studying liquid crystalline mesophases [11]. It has already been applied to determine different bulk properties of liquid

---

\*Corresponding author: barnavalentin@yahoo.com

crystals, such as bulk elastic constants [12-14], viscosities [15], helical twisting power [16], characteristics of the isotropic–nematic transition [17]. Furthermore, studies demonstrate the successful use of these methods for confined geometries analysis [18,19]. Another topic that is highly accessible for computer simulation is the investigation of topological defects in liquid crystals, such as disclinations [20,23], including those created in colloidal dispersions of small particles.

Combining molecular dynamics and Monte Carlo simulation, defect structures around an elongated colloidal particle embedded in a nematic liquid crystal host have already been studied [23]. In this manuscript, we propose for investigation the particular case for the molecular reconfiguration of a liquid crystal system composed of a nematic cell, when considering a bulk spherocylinder-like particle inclusion and an electric field is applied on the simulated domain.

## 2. Molecular Model and Simulation Method

We performed Monte Carlo simulations of a nematic liquid crystalline material in which we consider the existence of a spherocylinder-like nanoparticle in the presence of an applied electric field (for certain directions relative to the long axis of the spherocylinder). The simulation employs the generally used Lebwohl-Lasher model [24], where the liquid crystal molecules are considered as unit vectors (versors or spins) which occupy fixed positions in the sites of a cubic crystalline lattice. These versors are described by their cartesian components,  $\hat{e} = (e_x, e_y, e_z)$  and are free to rotate and interact with each other through an orientation dependent energy. The energy of interaction between versors with subscripts  $i$  and  $j$  is defined as:

$$U_{ij} = -\varepsilon_{ij}P_2(\cos \theta_{ij}) \quad (1)$$

In the above relation,  $P_2$  is the second rank Legendre polynomial and  $\theta_{ij}$  is the angle between the versors, obtained from their dot product,  $\cos \theta_{ij} = \hat{e}_i \cdot \hat{e}_j$ .  $\varepsilon_{ij}$  is a positive interaction constant for first order neighboring particles and zero otherwise.

The energy of interaction between molecules is invariant under an uniform rotation of all spins and, in this model, the bend, splay and twist elastic constants of the liquid crystal are considered equivalent [25–29].

In our model, the molecules' centers of mass are arranged in an ordered manner, yet not contradicting the fact that a liquid crystal is a fluid (*i.e.* there is no positional order of the molecules). In a real liquid crystal, the molecules arrange themselves in ordered domains; here each spin represents an ordered domain encompassing many molecules whose centers of mass are arbitrarily distributed [25, 29].

A significant advantage of using the Lebwohl-Lasher model, in contrast with other computational models presenting translational degrees of freedom, is the fact that spins' centers of mass are fixed, significantly reducing the computer simulation time. It was found that this system gives a realistic representation of a nematic liquid crystal having a first order phase transition at the scaled temperature  $T_{NI}^* = \frac{kT_{NI}}{\varepsilon} = 1.1232 \pm 0.0006$  [30,31].

An electric field,  $\vec{E}$ , applied to the simulated cell leads to an interaction of the spin  $i$  with this field [25,30]:

$$U_i = -\xi P_2(\hat{e}_i \cdot \hat{E}) \quad (2)$$

where  $\xi \sim \Delta\alpha E^2$  is a parameter describing the coupling between spin and the electric field and  $\hat{E}$  is the directional versor of the electric field [25].  $\Delta\alpha$  is the electrical polarizability anisotropy and its sign and magnitude determines the strength and direction of interaction between the spin and the applied electric field.

The total energy of the system is then [25]:

$$U = \sum_{i \neq j} U_{ij} + \sum_i U_i \quad (3)$$

The considered nematic liquid crystal that is used in the simulation is placed in a box of rectangular shape, with dimensions  $N_x \times N_y \times N_z$  in lattice spacing. In the middle of the box, we include a spherocylinder-like particle of length  $L$  and diameter  $D$ , as shown in Fig. 1.

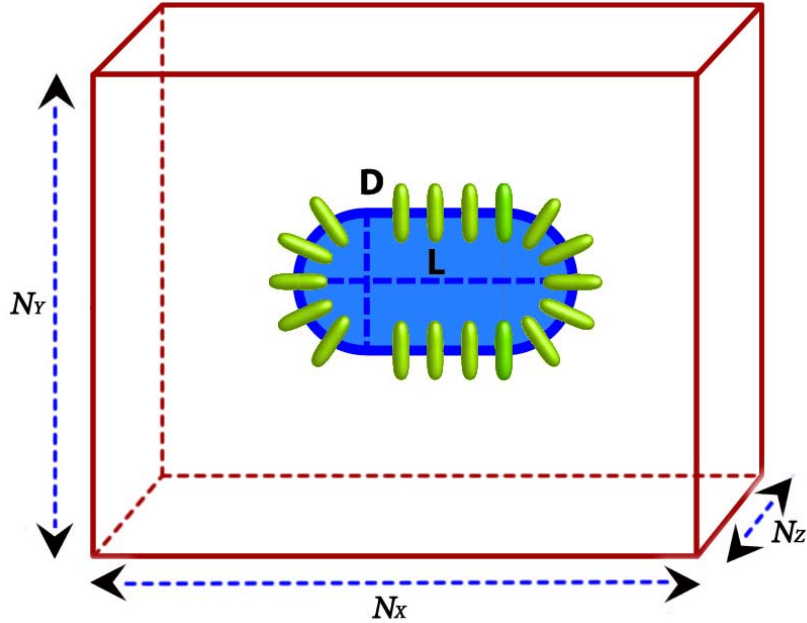


Fig. 1: Schematic representation of the simulated liquid crystal system with the integrated spherocylinder particle.

In all directions, we imposed periodic boundary conditions. The spins which are not situated in the vicinity of the particle interact with their neighbors through an interaction parameter,  $\epsilon_B$ , and are free to rotate inside their cells following a standard Monte Carlo procedure [8-11]. The anchoring of the molecules to the spherocylinder is accomplished by considering that it is made-up from fixed spins [22, 25-31]. These spins cannot rotate, but they can interact with other free spins through an interaction parameter,  $\epsilon_S$ . The orientation imposed by the walls of the spherocylinder is homeotropic, i.e. perpendicular to them: in the case of the hemispheres, the fixed spins are orientated in the direction of their centers and, for the cylindrical part, in the direction perpendicular to the long axis, as shown in Fig. 1. This interaction parameter describes the anchoring effects at the boundaries of the inclusion.

For temperatures bellow  $T_{NI}^*$  and in absence of the electric field, the competition between these orientational tendencies were studied using both Monte Carlo and Molecular Dynamics methods [22], resulting in an interesting distribution of the director field inside the simulated nematic cell. The classical way to describe the order of a liquid crystal is to use the scalar order parameter, which is defined with respect to a preferential axis [1, 32]:

$$S = \langle P_2(\cos \theta) \rangle = \frac{3\langle \cos^2 \theta - 1 \rangle}{2} \quad (4)$$

where  $\theta$  is the angle between a molecule and the favored axis and  $\langle \dots \rangle$  means the statistical average. The order parameter has the value 1 in the case in which all liquid crystal molecules are oriented along the preferential direction and 0 in for an isotropic liquid, that is the case of complete disorder.

As is intensely discussed in [8], in the computer simulation of a nematic, the bulk director changes slowly in space, typically to a length larger scale compared to the simulation box size, so a single director will apply to the entire sample. However, in our situation, due to the frustration imposed by the immersed nanoparticle, the changes of director in space is rapid and significant, as was already found in many similar situations [22, 25-30]. This is why, following the procedures from [25-31], we define in each point of the lattice a tensor order parameter:

$$Q_{\alpha\beta} = \frac{3}{2} \left( \langle e_{\alpha} e_{\beta} \rangle - \frac{1}{2} \delta_{\alpha\beta} \right) \quad (5)$$

where  $\alpha, \beta = x, y, z$ ,  $\delta_{\alpha\beta}$  is the Kronecker delta and  $\langle \dots \rangle$  means again the statistical average.

The diagonal components,  $Q_{XX}$ ,  $Q_{YY}$  and  $Q_{ZZ}$ , of the tensor order parameter represent the degree of order with respect the coordinate axis. The off-diagonal components,  $Q_{\alpha\beta}$ , represent the bending of the director in the corresponding plane. The values of the tensor order parameter are between  $-0.5$ , when the director is perpendicular to the corresponding direction, and  $1$ , when the director is perfectly parallel with the direction. In our simulations, we used relation (5) to calculate the components of the tensor as statistical averages for each cell. The obtained values are between these limits, while the value  $0$  meaning total disorder with respect the selected direction.

The largest positive eigenvalue of the tensor order parameter is the scalar order parameter and the corresponding eigenvector is the molecular director [8,33]. The absolute value of the difference between the remaining two eigenvalues of the order tensor parameter represents the biaxiality [34].

The Monte Carlo procedure used in our simulations was a standard one [8-11]: we randomly picked a free spin and rotated it with a small angle using the procedure from [9]. We calculated its energies in the old and in the new state and the move was accepted using the Metropolis acceptance criterion. The mechanism was repeated for 120,000 Monte Carlo cycles with 60,000 of them used for equilibration. During the simulation, we have dynamically adjusted the maximum rotation angle of the molecules, in order to have an acceptance ratio of 50%.

### 3. Results and discussion

The described system was used to simulate the behavior of a nematic liquid crystal, the molecular order being influenced by the spherocylinder inclusion in competition with the alignment imposed by the applied electric field. The size of the simulation box was  $N_x = 64$ ,  $N_y = 48$ ,  $N_z = 48$  in lattice spacings. The length of the spherocylinder was  $L = 32$  and its diameter  $D = 16$ . Because spins located inside the nanoparticle are fixed, the number of free spins was 141,952 and a Monte Carlo cycle consisted of 141,952 attempted moves.

The proportions of the simulated box versus the spherocylinder were selected in such way, for avoiding as much as possible the finite geometrical effects.

The coupling interaction constant between free spins was  $\varepsilon_B = 1$  and between a free spin and a fixed one was  $\varepsilon_S = 1.5$ . We employed this very large value for the anchoring constant in order to emphasize the competition between the alignment of the liquid crystal molecules in electric field, versus the effects of the boundary conditions on the walls of the immersed particle.

In order to have a comparison with the results of [22] we performed a first set of Monte Carlo simulations in the absence of the electric field, at a reduced temperature  $T^* = 1.0$ . In this situation, our material is situated in the nematic phase and the reduced temperature corresponds to the room temperature for the 5CB nematic liquid crystal [30].

In Fig. 2, we represented the surface plot of the order parameter  $S$  in the plane  $x = 31$ , *i.e.* on a transversal section near the middle of the spherocylinder.

Sufficiently far away from the nanoparticle, the order parameter is approximately  $0.6$ , which is in good agreement with the value of the bulk order parameter found for the Lebwohl-Lasher model [27, 30] and the same as the value from [22]. As expected, very close to the walls of the spherocylinder, the scalar order parameter has larger values, mainly due to the imposed very strong anchoring. The exceptions are the regions from figures 2 and 3, where the order parameter decreases to approximately  $-0.25$ . In these points, we also calculated the biaxiality of the system,

finding a value of approximately 0.25, both of them very close to the values from [22]. This behavior was also found in reference [22] and these regions correspond to a pair of  $-\frac{1}{2}$  defects. The fact that these defects are situated close to the diagonal of the simulation box is explained to be a result of the repulsion between them, resulting in the maximization of the distance.

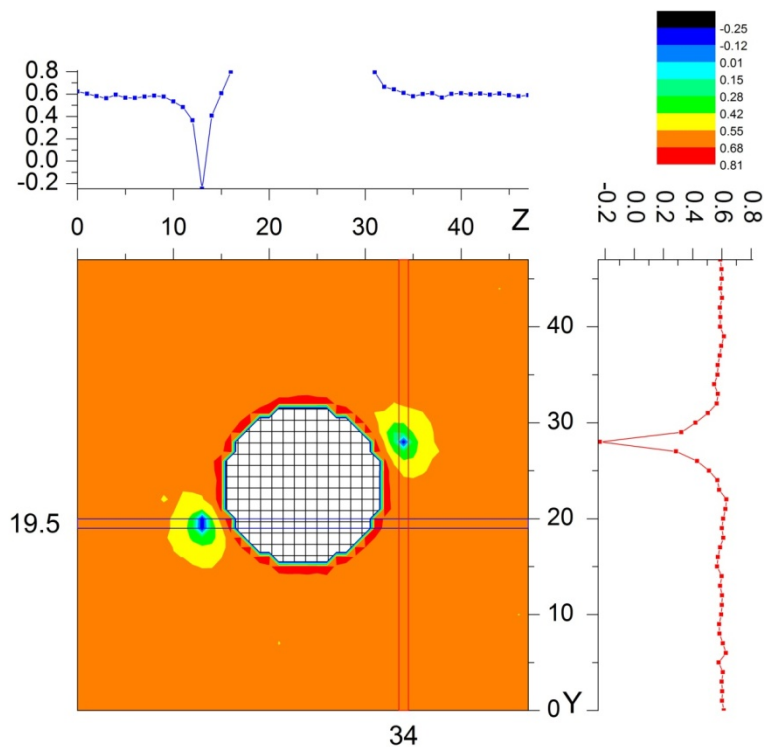


Fig. 2: Surface plot of the order parameter  $S$  in the plane  $x = 31$ .

Fig. 3 represents the same parameter, but in a longitudinal section of the spherocylinder, in the plane  $z = 24$ . We again found the opposite regions where the system become biaxial, once more situated close to the diagonal of the longitudinal section.

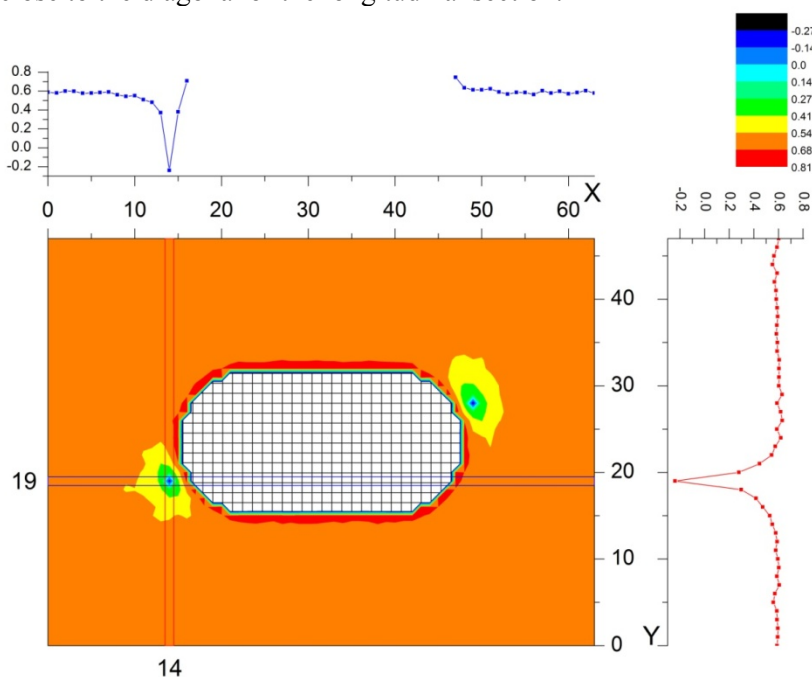


Fig. 3: Surface plot of the order parameter  $S$  in the plane  $z = 24$ .

By analyzing the whole data set, we found a closed oblate disclination line situated near the diagonal plane of the simulation box. It had a shape of a section of a spherocylinder and corresponds to the Saturn ring line reported in [23] for the case of a sphere.

We repeated the simulation for a reduced temperature  $T^* = 1.4$ , above the nematic isotropic transition, and the obtained order parameter was very close to zero, indicating the absence of the order.

In the presence of an applied electric field, in the case of the positive dielectric anisotropy liquid crystal, the nematic director tends to align the spins along its direction, competing with the direction imposed by the immersed spherocylinder.

The following set of results represent the simulations with an electric field applied parallel with respect to the long axis of the spherocylinder (*i.e.* in the OX direction) and with  $\xi = 0.1$ , corresponding to a positive dielectric anisotropy of the nematic. As observed from figures 4 and 5, where are represented the same sections as above, the scenery of the nematic director is greatly modified. Firstly, the disclination line is displaced from the hemispherical cap of the spherocylinder toward its cylindrical part, becoming circular, while situated in the YZ plane. The value of S for the disclination line is roughly  $-0.27$  and the calculated biaxiality is  $\cong 0.25$ .

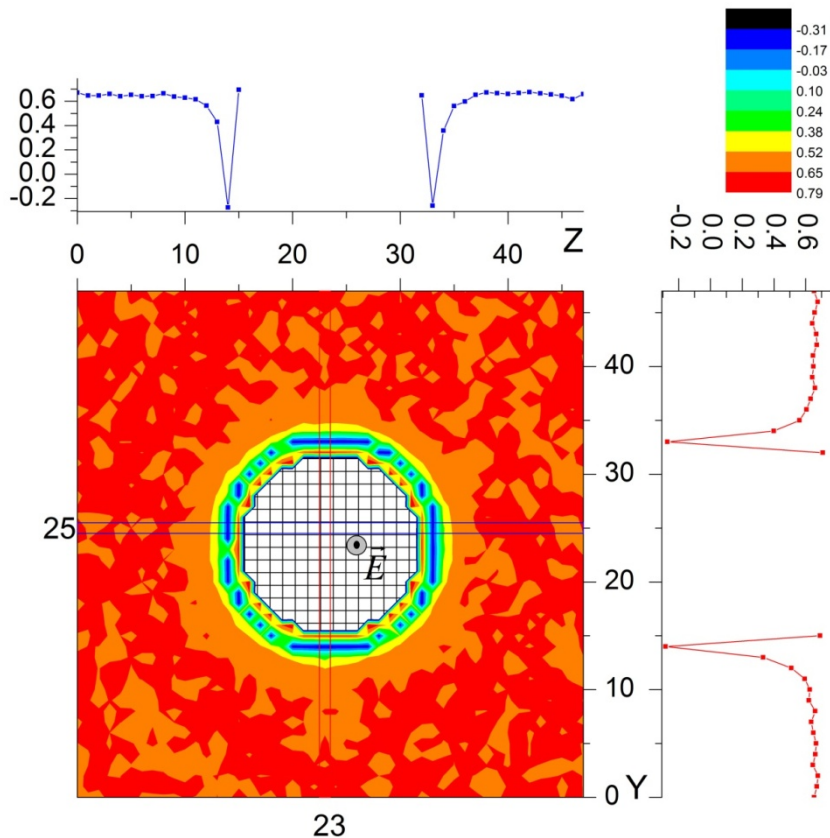


Fig. 4: Surface plot of the order parameter  $S$  in the plane  $x = 31$ , with an applied electric field ( $\xi = 0.1$ ) along the OX axis.

Near the caps of the spherocylinder the electric field is parallel with the direction imposed by the anchoring conditions and the order level is increased to 0.7 (compared to 0.65 value for the bulk).

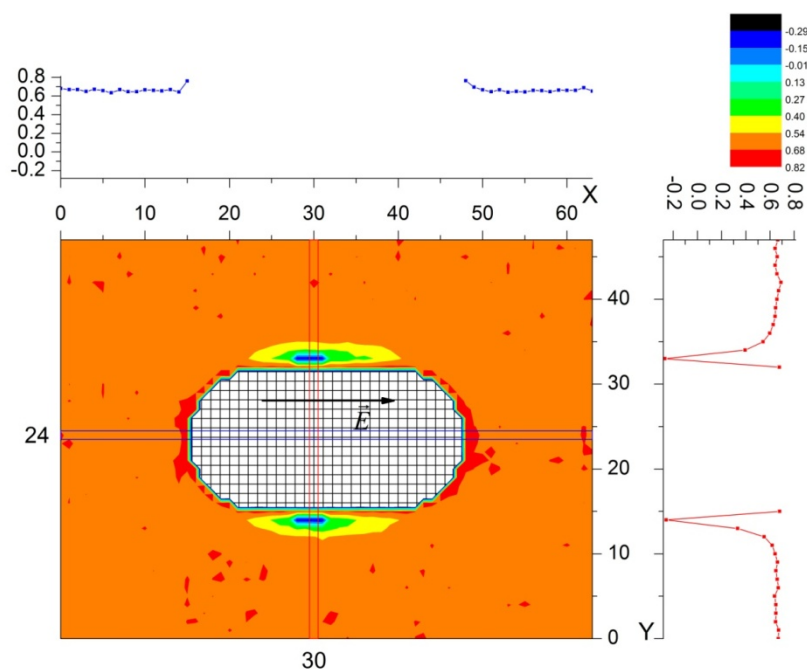


Fig. 5: Surface plot of the order parameter  $S$  in the plane  $z = 24$  with an applied electric field ( $\xi = 0.1$ ) along the  $OX$  axis.

Following the procedure from [25,35] we define a field order parameter that describes the order of the system in the direction of the applied field in each point of the lattice:

$$P_2^E = P_2(\hat{e} \cdot \hat{E}) \quad (6)$$

The representation of the field order parameter is shown in figure 6. In the bulk, as expected, the molecules align parallel with the direction of field along the  $OX$  axis, the typical value of the field order parameter being  $\cong 0.66$ . We also have inspected the diagonal components of the tensor order parameter and we found:  $Q_{XX} \cong 0.67$ ,  $Q_{YY} \cong -0.33$  and  $Q_{ZZ} \cong -0.33$ . These values lead to the conclusion that, in the bulk and sufficiently away from spherocylinder, the molecular director is parallel with  $OX$  axis and perpendicular on  $OY$  and  $OZ$ . In the immediate vicinity of the cylindrical part of the spherocylinder, the alignment of molecules is dictated by anchoring conditions: they are parallel with the radial direction towards the axis of the spherocylinder (which is perpendicular to the  $OX$  axis).

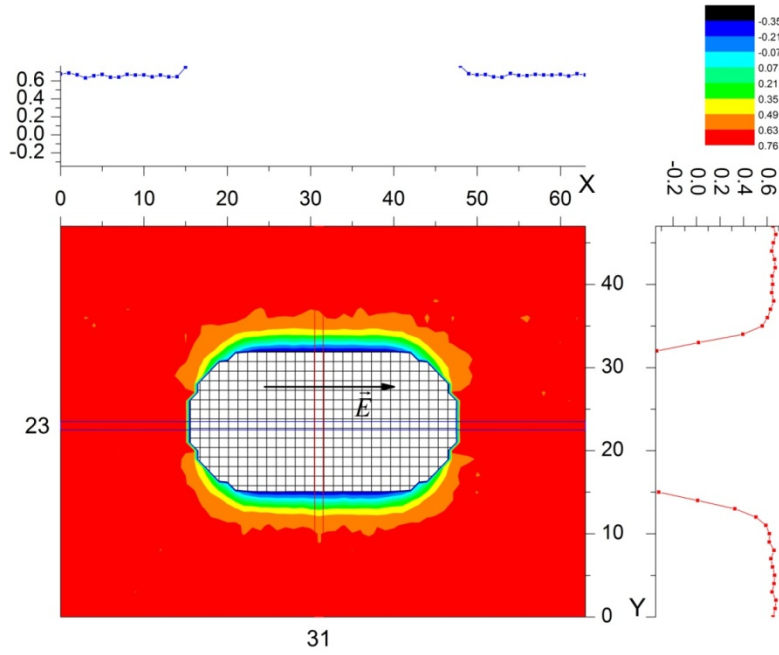


Fig. 6: Surface plot of the field order parameter in the plane  $z = 24$  with field an applied electric ( $\xi = 0.1$ ) along  $OX$  axis.

Therefore, if the electric field is along the  $OX$  axis, the Saturn ring corresponding to the disclination line is situated in the  $YZ$  plane.

If a field with the same parameter  $\xi = 0.1$  is applied along  $OY$ , the situation is changed: this time, the disclination line is situated in the plane  $XZ$ , its shape being a longitudinal section of a spherocylinder, as in figures 7 and 8.

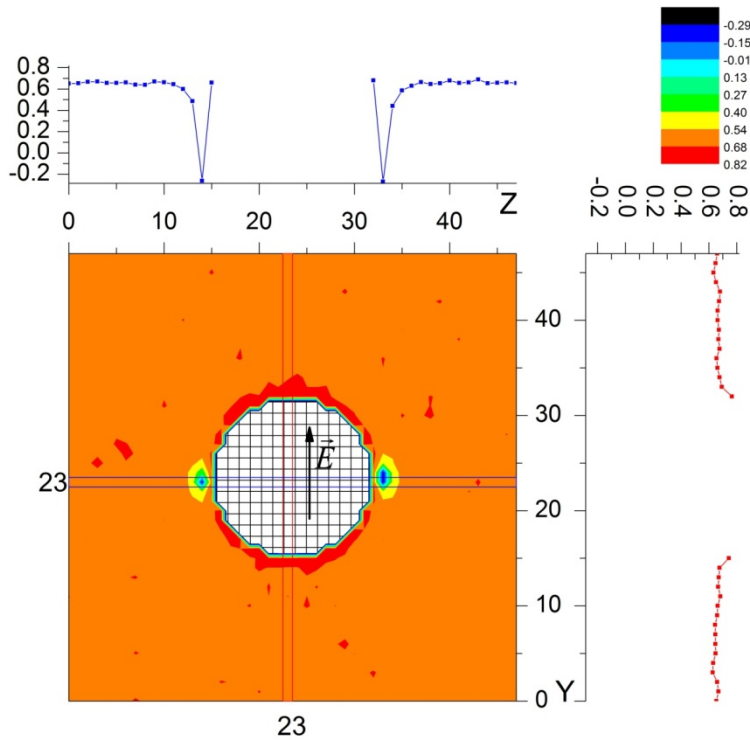


Fig. 7: Surface plot of the order parameter  $S$  in the plane  $x = 31$  with an applied electric field ( $\xi = 0.1$ ) along  $OY$  axis.

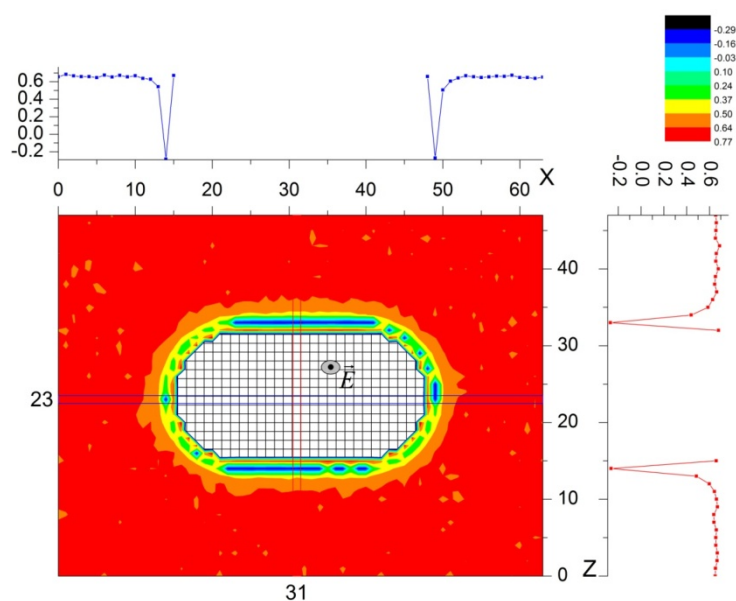


Fig. 8: Surface plot of the order parameter  $S$  in the plane  $y = 31$  with an applied electric field ( $\xi = 0.1$ ) along  $OY$  axis.

In the bulk, sufficiently away from the spherocylinder, the field order parameter value is again  $\cong 0.66$  and the diagonal components of the tensor order parameter are:  $Q_{XX} \cong -0.32$ ,  $Q_{YY} \cong 0.65$  and  $Q_{ZZ} \cong -0.33$ . It follows that, in this case, the molecular director is parallel with  $OY$  axis and perpendicular on  $OX$  and  $OZ$ . In the disclination line, the value of  $S$  is approximately  $-0.28$  and the biaxiality is  $\cong 0.25$ .

The main conclusion we may draw is that the existence of an electric field aligns the molecules on its direction while the disclination line is displaced, giving rise to a Saturn ring in a plane perpendicular to the field direction.

In order to prove this assertion, we repeated the simulation with an external electric field applied on the diagonal planes of the simulation cell. As it is shown in figures 9 and 10, in both situations, the disclination line is moved in such a way that its plane is perpendicular to the electric field.

For the situation in figure 10, a bulk molecule has the components of the tensor order parameter  $Q_{XX} \cong 0.26$ ,  $Q_{YY} \cong 0.06$  and  $Q_{ZZ} \cong -0.33$ , whereas the field order parameter is the same as before,  $\cong 0.66$ . It follows that molecules are oriented along the electric field, having the main component along  $OX$  axis and perpendicular to the  $OZ$  axis. For the disclination line, we find that  $S$  is around  $-0.27$  and the biaxiality is  $\cong 0.19$ .

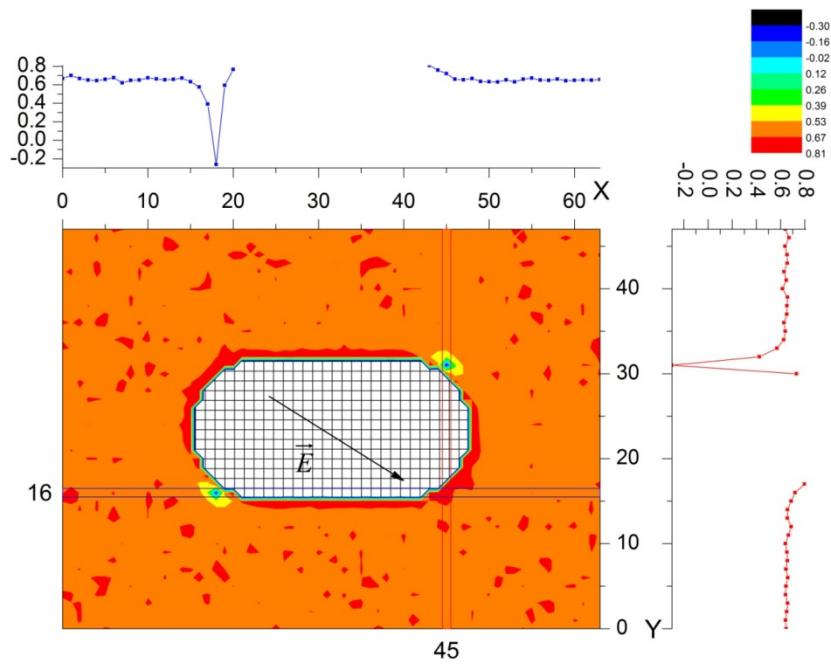


Fig. 9: Surface plot of the order parameter  $S$  in the plane  $z = 23$  with field  $\xi = 0.1$  along main diagonal plane of the simulated cell.

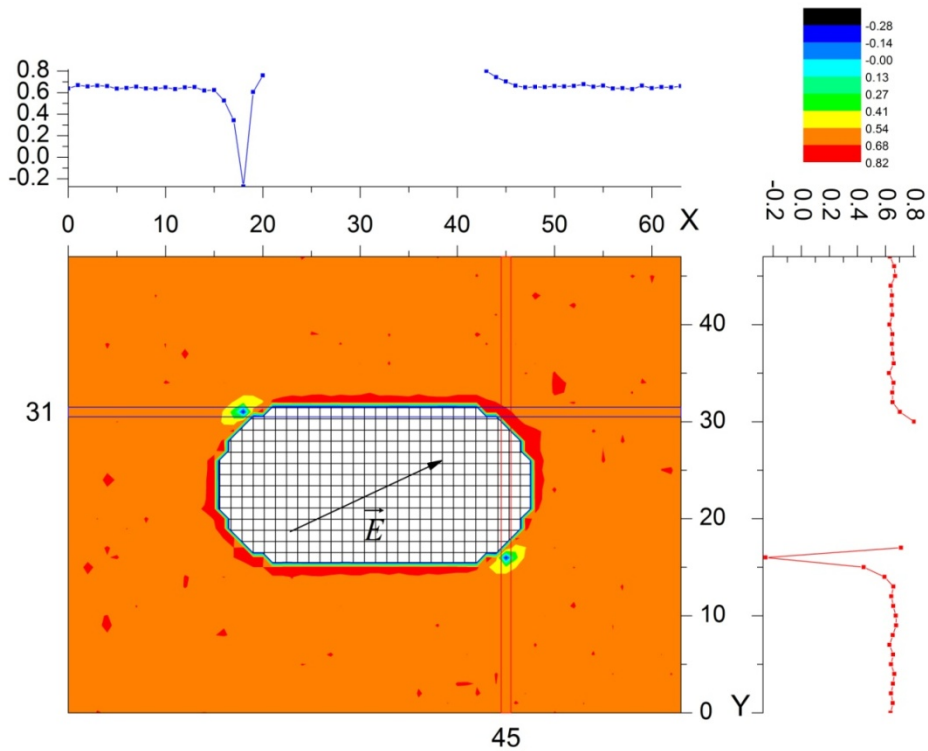


Fig. 10: Surface plot of the order parameter  $S$  in the plane  $z = 23$  with field  $\xi = 0.1$  along secondary diagonal plane of the simulated cell.

These results demonstrate that the electric field is reordering the molecules in such a way that the Saturn ring disclination line is displaced until its plane is perpendicular to the electric field direction.

We also performed a series of simulations with increasing values of the electric field oriented parallel with the long side of the spherocylindrical nanoparticle. At very low values of the

electric field the disclination line plane is slightly displaced from its original position, finding a threshold value  $\xi = 0.03$  when this plane becomes perpendicular on the field direction.

However, the further increasing of the electric field intensity results in finally destroying the disclination line. We found that, for a value above  $\xi = 0.75$ , the disclination line vanishes and the order in the entire simulation cell become uniaxial.

The situation is somewhat similar with the results from [35] where is explained that this behaviour is due to the Fréedericksz transitions of a liquid crystal in one-constant approximation. In our work, the interaction potential of the Lebwohl-Lasher model from equation (1) is isotropic in space and we cannot make a distinction between splay and twist deformations.

#### 4. Conclusions

Computer simulations are extremely valuable tools for investigating properties of systems for which behavior is sometimes very difficult to predict by using exact theoretical relations.

By means of Monte Carlo simulation of the Lebwohl-Lasher model we investigated the properties of a nematic liquid crystal hosting inside a spherocylindrical nanoparticle.

We considered first the situation from [22] and we retrieved the presence of a disclination line with the shape of the Saturn ring defect. We demonstrated that the order parameter of the system is strongly influenced by the presence of the spherocylindrical inclusion.

We also established that the geometry of the system plays a central role in determining the orientation of the nematic liquid crystal molecules, but the existence of a weak external perturbation (i.e. electric field) may further modify the map of the order parameter.

By applying an electric field on the simulation cell, the molecules in the bulk are primarily oriented parallel with the field direction and the disclination line is shifted until its plane is perpendicular on the field.

We consider that the investigated nematic liquid crystal domain presenting a spherocylindrical nanoparticle inclusion represents an attractive confinement system, both from theoretical and practical point of view, and could resolve many questions regarding special boundary anchoring conditions, molecular distribution and optical behaviour of these materials in complex geometries.

#### Acknowledgements

The research work was supported from the Romanian national projects CNCSIS TE 225-96/2010 and ID-PCE-2011/3/1007.

#### References

- [1] P.G. de Gennes, J. Prost, *The Physics of Liquid Crystals*, Oxford University Press, New York (1995).
- [2] L.M. Blinov, V.G. Chigrinov, *Electrooptic Effects in Liquid Crystal Materials*, Springer, New York, (1993).
- [3] A.K. Bhowmik, Z. Li, P. J. Bos (Eds.), *Mobile Displays: Technology and Applications* (Wiley Series in Display Technology), Wiley, Chicester (2008).
- [4] S.J. Woltman, G.D. Jay, G.P. Crawford, *Liquid Crystals: Frontiers in Biomedical Applications*, World Scientific Publishing Company, Singapore (2007).
- [5] Q. Li, *Liquid Crystals Beyond Displays: Chemistry, Physics, and Applications*, Wiley, New Jersey (2012).
- [6] G. Lombardo, H. Ayeb, R. Barberi, *Phys. Rev. E*, **77**, 051708 (2008).
- [7] A. Amoddeo, R. Barberi, G. Lombardo, *Comput. Math. Appl.*, **60**, 2239–2252 (2010).
- [8] M. P. Allen, D. J. Tildesley, *Computer Simulation of Liquids*, Oxford University Press, Oxford (1989).

- [9] D. Frenkel, B. Smit, *Understanding Molecular Simulation: From Algorithms to Applications*, Academic Press, New York (2001).
- [10] D. P. Landau, K. Binder, *A Guide to Monte Carlo Simulations in Statistical Physics*, Cambridge University Press, Cambridge (2000).
- [11] P. Pasini, C. Zannoni, S. Žumer (Eds.), *Computer Simulations of Liquid Crystals and Polymers*, Kluwer Academic Publishers, Dordrecht (2005).
- [12] J. Stelzer, L. Longa, H. R. Trebin, *J. Chem. Phys.*, **103**, 3098–3107 (1995).
- [13] J. Stelzer, L. Longa, H. R. Trebin, *Mol. Cryst. Liq. Cryst. Sci. Technol. Sect. A*, **262**, 455–461 (1995).
- [14] J. Stelzer, H.-R. Trebin, L. Longa, *J. Chem. Phys.*, **107**, 1295–1296 (1997).
- [15] S. Sarman, *J. Chem. Phys.*, **108**, 7909–7916 (1998).
- [16] R. Memmer, F. Janssen, *J. Chem. Soc. Faraday Trans.*, **94**, 267–276 (1998).
- [17] M. P. Allen, *J. Chem. Phys.*, **112**, 5447–5453 (2000).
- [18] M. P. Allen, *Molec. Phys.*, **96**, 1391–1397 (1999).
- [19] D. Andrienko, G. Germano, M. P. Allen, *Phys. Rev. E*, **62**, 6688–6693 (2000).
- [20] D. Andrienko, M. P. Allen, *Phys. Rev. E*, **61**, 504–510 (2000).
- [21] S. D. Hudson, R. G. Larson, *Phys. Rev. Lett.*, **70**, 2916–2919 (1993).
- [22] D. Andrienko, M.P. Allen, G. Skacej, S. Žumer, *Phys. Rev. E*, **65**(4), 041702-041702, (2002).
- [23] S. Grollau, N.L. Abbott, J.J. de Pablo, *Phys. Rev. E*, **67**(1 Pt 1), 011702, (2003).
- [24] P.A. Lebwohl, G. Lasher, *Phys. Rev. A*, **6**, 426–429 (1972).
- [25] N. Scaramuzza, C. Berlic, E. Barna, G. Strangi, V. Barna, A. Th. Ionescu, *J. Phys. Chem. B*, **108**, 3207–3210 (2004).
- [26] C. Berlic, V. Barna, *Opt. Express*, **18**(23), 23646 (2010).
- [27] A. M. Smondyrev, R. A. Pelcovits, *Liq. Cryst.*, **26**, 235–240 (1999).
- [28] C. Berlic, E. Barna, C. Ciucu, *Journal of Optoelectronics and Advanced Materials* **9**, 3854-3859 (2007).
- [29] C. Berlic, V. Barna, *Journal of Optoelectronics and Advanced Materials*, **12**, 1427 - 1432 (2010).
- [30] E. Berggren, C. Zannoni, C. Chiccoli, P. Pasini, F. Semeria, *Int. J. Modern Physics C* **6**, 135-141 (1995).
- [31] C. Chiccoli, P. Pasini, A. Sarlah, C. Zannoni, S. Žumer, *Phys. Rev. E* **67**, 050703 (2003).
- [32] S. Chandrasekhar, *Liquid Crystals*, Cambridge University Press, Cambridge (1994).
- [33] G.R. Luckhurst, G.W. Gray, *The Molecular Physics of Liquid Crystals*, Academic Press, New York (1979).
- [34] C. Berlic, V. Barna, *Mol. Cryst. Liq. Cryst.*, **549**, 140–149, (2011).
- [35] C. Chiccoli, P. Pasini, S. Guzzetti, C. Zannoni, *Mol. Cryst. Liq. Cryst.*, **360**, 119, (2001).
- [36] C. Chiccoli, P. Pasini, G. Skacej, C. Zannoni, S. Žumer, *Phys Rev E: Stat. Nonlin. Soft Matter Phys.*, **67** (1 Pt 1), 010701, (2003).